Astronomy and Space Science: Open Access
Received: Oct 21, 2016, Accepted: Feb 11, 2017, Published: Feb 16, 2017
Astron Space Sci, Volume 3, Issue 1
http://crescopublications.org/pdf/ASSOA/ASSOA-3-010.pdf
Article Number: ASSOA-3-010

Research Article Open Access

Study of Electrostatic Ion-Cyclotron Instability with Multi-Component Anisotropic Plasma around Plasma Sheet Boundary Layer Region

BD Raikwar*, P. Varma and MS Tiwari

Department of Physics, Dr. H.S. Gour Vishwavidyalaya, Sagar (M.P.) 470003, India

***Corresponding Author:** BD Raikwar, Department of Physics, Dr. H.S. Gour Vishwavidyalaya, Sagar (M.P.) 470003, India, E-mail: bhagwandr.90@gmail.com

Citation: BD Raikwar, P Varma and MS Tiwari (2017) Study of Electrostatic Ion-Cyclotron Instability with Multi-Component Anisotropic Plasma around Plasma Sheet Boundary Layer Region. Astron Space Sci 3: 010.

Abstract

Electrostatic ion-cyclotron (EIC) instabilities are investigated with multi-ion (H+, He+ and O+) anisotropic plasma by using particle aspect analysis. The variation with perpendicular wave number for resonant energy and growth rate with general distribution function are studied. The whole plasma is considered to consist of resonant and non-resonant particles. The resonant particles participate in energy exchange processes, whereas the non-resonant particles support the oscillatory motion of the wave. The wave is assumed to propagate obliquely to the static magnetic field. It is found that the temperature anisotropy enhances the transverse and parallel resonant energy of particles and growth rate of the wave. The study may explain the EIC waves observed in plasma sheet boundary layer region. The results are interpreted for the space plasma parameters appropriate to the plasma sheet boundary layer region around the earth's magnetosphere.

Keywords: Electrostatic ion-cyclotron waves; Multi-component plasma; Particle aspect approach; Resonant particles; Non-resonant particles; Temperature anisotropy; Plasma sheet boundary layer region.

1. Introduction

The stability of EIC wave in plasma consisting of isotropic hydrogen ions and temperature-anisotropic positively and negatively charged oxygen ions, with the electrons drifting parallel to the magnetic field was studied by Kurian et al. [1]. Analytical expressions derived for the frequency and growth/damping rate around the first harmonic of both hydrogen and oxygen ion gyro frequencies reveal that they are dependent on the densities and temperatures of all species of ions. The waves are driven by the electron drift parallel to the magnetic field; the temperature anisotropy of the oxygen ions slightly enhances the growth rates for small values of temperature anisotropies Kurian et al. [1]. The nightside auroral region maps to the plasma sheet. Generator regions which are important for auroral activity are therefore expected to exist in and near the plasma sheet. Several regions in the

plasma sheet, the low-latitude boundary layer and the plasma sheet boundary layer have been suggested to host auroral generators. Paschmann et al. [2] have presented an overview on this.

It is well established that magnetopause reconnection for southward IMF plays a central role in controlling magnetospheric structures and dynamics; relatively little is understood concerning what magnetopause process a global impact in terms of the mass, momentum has or energy transport under northward IMF. Observations show that cool and dense plasmas of solar wind origin, loaded into the plasma sheet under northward IMF, can eventually have access to the inner magnetosphere [3], and such preconditioning during northward IMF periods has a large impact on magnetospheric activities such as geomagnetic storms [4].

The plasma sheet boundary layer (PSBL) facilitates favourable conditions for wave-particle interactions, and in fact the broadband electrostatic and electromagnetic waves are almost always observed. Recent Cluster studies reported properties of multiple energy-dispersed ion structures in the plasma sheet boundary layer (PSBL) that showed substructure with several well separated ion beamlets, covering energies from 3 keV up to 100 keV [5]. They described observations of phenomena which are associated with energy dispersed ion structures in the PSBL for two events using a comprehensive set of instruments on-board Cluster. Both events have previously been investigated with regard to properties and generation mechanism of the dispersed ion structures. Cluster observations show that energy dispersed ions in the PSBL energetically drive the heating of ion outflows forming ion conics, the field-aligned acceleration of electrons, and the generation of perpendicular electric fields and ELF turbulence [5].

In this paper, we study how ion temperature anisotropy can affect the threshold conditions; we have also studied a systematic and detailed investigation of EIC waves in multi-component plasma in plasma sheet boundary layer region for magnetosphere like plasma parameters with the purpose of attaining a more complete understanding of their relative importance. We are using particle aspect approach. The advantage of present approach is to its suitability for dealing with dynamics of particles in PSBL region involving the heating, acceleration and energy exchange by wave particle resonant interaction.

In section 1 we represent introduction. Section 2 represents the basic trajectories following the velocities of the charged particles. Section 3 describes the dispersion relation of EIC waves. In section 4 energy balance and growth rate of EIC waves with multicomponent plasma are evaluated. Section 5 describes the result and discussions of the study.

2. Basic Assumptions:

An EIC wave is assumed to start at t = 0 when the resonant particles are not disturbed. The trajectories of particles are then evaluated within the framework of linear theory [6 - 9]. The wave is assumed to have the form:

$$K \parallel E, k = (k_{\perp}, 0, k_{\Pi}), E = (E_X, 0, E_Z)$$

With

$$E_X(r,t) = E_1 \cos(k_{\perp} x + k_{\Pi} z - \omega t),$$
$$E_Z(r,t) = \kappa E_1 \cos(k_{\perp} x + k_{\Pi} z - \omega t)$$

And

$$\kappa = \left(\frac{k_{\Pi}}{k_{\perp}} \right) < 1$$

The amplitude E_1 is slowly varying function of t i.e.

$$\frac{1}{E_1}\left(\frac{dE_1}{dt}\right) << \omega$$

The EIC instability in the system of hot electrons and hot ions is considered under the condition:

$$V_{T\Pi\alpha} < \left|\frac{\omega - \lambda\Omega_\alpha}{k_\Pi}\right| << V_{T\Pi e} \text{ and } k_\perp{}^2\rho_e{}^2 << k_\perp{}^2\rho_\alpha{}^2 \sim 1$$

Where $V_{T\Pi\alpha,e}$ is the thermal velocity of the ions and electrons, respectively along the magnetic field, Ω_α is the ion-cyclotron frequency. $\lambda = 1,2,....$ represent the harmonics of the wave, $\rho_{i,e}$ is the mean gyro-radii of the ions and electrons, respectively, k_Π and $k_\perp$ are the components of the wave vector along and across the magnetic field and ω represents the wave frequency.

2.1 Trajectories and velocities of charged particles;

The trajectories of particles are evaluated within the framework of linear theory. The equation of motion of a particle is given by:

$$m\left(\frac{dv}{dt}\right) = q\left[E + (\frac{1}{c})v \times B_0\right] \qquad (1)$$

If E is considered to be a small perturbation i.e., $E = E_1$, velocity v can be expressed in terms of unperturbed velocity V and perturbed velocity u.

The quasi-neutrality condition yields to the equation:

$$n_e = n_{H^+} + n_{O^+} + n_{He^+}$$

3. Dispersion Relation:

The Poisson equation is,

$$\nabla.E = -k_\perp(1+\kappa^2)E_1 \sin(k.r - \omega t) = 4\pi e(n_i - n_e), \qquad (2)$$

Where $n_{i,e}$ is integrated perturbed density of the non-resonant particles of the respective species given by,

$$n_{\alpha,e} = \mp\int dvN(v)\frac{eE_1k_\perp}{m_{\alpha,e}}\sum_{nl}\left\{J_n(\mu)J_l(\mu)\times\left(\frac{1}{\wedge^2{}_n - \Omega_\alpha{}^2} + \frac{\kappa^2}{\wedge^2}\right)\sin\chi_{nl}\right\}_{i,e} \qquad (3)$$

Where $\mu = \frac{k_\perp V_\perp}{\Omega_{\alpha,e}}, \wedge_n = k_\Pi V_\Pi - \omega + n\Omega_{i,e}$ and $\chi_{nl} = k.r - \omega t + (n-l)(\Omega_\alpha l - \theta)$

Where, $\alpha = H,^+ He^+, O^+$

Using expression for unperturbed density for the non-resonant ions [6 - 9] and the integrated perturbed densities for the non-resonant particles is derived as

$$n_e \cong \left(\frac{1}{\kappa_\perp {d_{\|e}}^2}\right)\frac{E_1}{4\pi e}\sin(k.r-\omega t) \quad \text{and} \quad n_i \cong \frac{k_\perp \kappa^2 {\omega^2}_{p\alpha}}{[\omega-\lambda\Omega_\alpha]}\left\langle {J_\lambda}^2\right\rangle \frac{E_1}{4\pi e}\sin(k.r-\omega t)$$

$$\left\langle {J^2}_\lambda\right\rangle = \int_0^\infty 2\pi V_\perp dV_\perp {J^2}_l(\mu) f_{\perp\alpha}(V_\perp)$$

Where, $\alpha = H,^+ He^+, O^+$ $\quad {\omega_{p\alpha}}^2 = \dfrac{4\pi N_\alpha e^2}{m_\alpha}$ is required plasma frequency for the multi ions and N_α the multi ions plasma density. Then the dispersion relation is,

$$1+\left(\frac{1}{1+\kappa}\right)\left(\frac{1}{{k_\perp}^2 {d^2}_{\Pi e}}\right)-\left(\frac{\kappa^2}{1+\kappa}\right)+\left(\frac{{\omega_{p\alpha}}^2}{(\omega-\lambda\Omega\alpha)^2}\right)<\left({J^2}_{\lambda-1}-{J^2}_{\lambda+1}\right)>\cong 0 \qquad (4)$$

For λ =1, $\left\langle\left({J^2}_0+{J^2}_2\right)\right\rangle = 1-(j+1)\dfrac{{k^2}_\perp {\rho^2}_\alpha}{2}$;

$$\left\langle\left(J_0+J_2\right)^2\right\rangle = 1-\frac{1}{2}(j+1)\frac{{k^2}_\perp {\rho^2}_\alpha}{2}$$

For J = 0 this dispersion relation reduces to that given by Terashima [10].

4. Energy Balance and Growth Rate:

The wave energy per unit wavelength can be defined as

$$W_w = \frac{\lambda {E_1}^2}{8\pi} + W_e + W_\alpha \text{ where,}$$

$$W_{\alpha,e} = \int_0^\lambda ds \int dV \frac{m_{e,\alpha}}{2}\left\{(N+n_1)(V+u)^2 - NV^2\right\}_{\alpha,e},$$

$$W_w \approx \frac{\lambda {E^2}_1}{8\pi} + \frac{\lambda {E^2}_1}{16\pi}\frac{{\omega^2}_{p\alpha}}{\left\{\omega-\lambda\Omega_\alpha\right\}^2}\kappa^2\frac{1}{2}\left\langle {J_{\lambda-1}}^2 + {J_{\lambda+1}}^2\right\rangle + \frac{\lambda {E^2}_1}{16\pi}\left(\frac{1}{{k^2}_\perp {d^2}_{\Pi e}}\right) \qquad (5)$$

The changes in energy of the resonant particles are,

$$W_r = \sum_{i,e}(W_{r\perp} + W_{r\Pi})$$

$$W_{r\perp} = \int_0^\lambda ds \int_0^\infty V_\perp dV_\perp \int_0^{2\theta} d\theta \int_{v_r-\Delta r}^{v_r+\Delta r} dV_\Pi \frac{m_\alpha}{2}\left\{(N+n_1)(V_\perp+u_\perp)^2 - N{V_\perp}^2\right\}, \qquad (6)$$

$$W_{r\Pi} = \int_0^{\lambda} ds \int_0^{\infty} V_{\Pi} dV_{\Pi} \int_0^{2\theta} d\theta \int_{v_r-\Delta r}^{v_r+\Delta r} dV_{\Pi} \frac{m_{\alpha}}{2} \left\{ (N+n_1)(V_{\Pi}+u_{\Pi})^2 - N{V_{\Pi}}^2 \right\} \tag{7}$$

For the resonant particles $\delta = 1$ and the resonant velocity V_r defined as

$$V_r = \frac{\omega - l\Omega_i}{k_{\Pi}},$$

$$W_{r\perp} = \left(\frac{\lambda {E^2}_1}{8\pi} \right) \left(\frac{{\omega^2}_{p\alpha}}{{\Omega^2}_{\alpha}} \right) \left(\frac{\omega}{k_{\Pi} V_{th\alpha}} \right) \frac{\Omega_{\alpha} t}{\sqrt{2\pi}} \exp\left\{ -\frac{1}{2} \left(\frac{\omega}{k_{\Pi} V_{th\alpha}} \right)^2 \left(1 - \frac{\lambda\Omega_{\alpha}}{\omega} \right)^2 \right\}$$

$$\times \frac{1}{2} \left\langle {J_{\lambda-1}}^2 + {J_{\lambda+1}}^2 \right\rangle \left[1 - \left(\frac{R\left(\frac{\lambda\Omega_{\alpha}}{\omega} - 1 \right)}{\frac{\lambda\Omega_{\alpha}}{\omega}} \right) \frac{T_{\perp\alpha}}{T_{\Pi\alpha}} \right] \tag{8}$$

$$W_{r\Pi} = \left(\frac{\lambda {E^2}_1}{8\pi} \right) \left(\frac{{\omega^2}_{p\alpha}}{{\Omega^2}_{\alpha}} \right) \left(\frac{\omega}{k_{\Pi} V_{th\alpha}} \right) \frac{\Omega_{\alpha} t}{\sqrt{2\pi}} \exp\left\{ -\frac{1}{2} \left(\frac{\omega}{k_{\Pi} V_{th\alpha}} \right)^2 \left(1 - \frac{\lambda\Omega_{\alpha}}{\omega} \right)^2 \right\}$$

$$\times \frac{1}{2} \left\langle (J_{\lambda-1} + J_{\lambda+1})^2 \right\rangle \left[\frac{\left(1 - \frac{\lambda\Omega_{\alpha}}{\omega} \right)}{\frac{\lambda\Omega_{\alpha}}{\omega}} \right] \frac{T_{\perp\alpha}}{T_{\Pi\alpha}} \tag{9}$$

Where,

$$R = \frac{(J_{l+1} + J_{l-1})^2}{\langle {J_{l+1}}^2 + {J_{l-1}}^2 \rangle}$$

$$\langle {J_l}^2(\mu) \rangle \approx \langle \left(J_{l+1}(\mu) + J_{l-1}(\mu) \right)^2 \rangle ({\mu^2}/{4l^2})$$

Using the law of conservation of energy the growth rate is obtained to be

$$\left| \frac{d{W^{\alpha}}_{r\perp}}{dt} \right| \rangle \frac{d{W^{\alpha}}_{r\Pi}}{dt}$$

Hence the growth rate is,

$$\frac{\gamma}{\omega} = \sqrt{\frac{\pi}{2}} \left(\frac{\omega}{k_{\Pi} V_{th\alpha}} \right) \left(1 - \frac{\lambda\Omega_{\alpha}}{\omega} \right)^2 \exp\left\{ -\frac{1}{2} \left(\frac{\omega}{k_{\Pi} V_{th\alpha}} \right)^2 \left(1 - \frac{\lambda\Omega_{\alpha}}{\omega} \right)^2 \right\}$$

$$\times \left[R \left(\frac{\frac{\lambda\Omega_{\alpha}}{\omega} - 1}{\frac{\lambda\Omega_{\alpha}}{\omega}} \right) \frac{T_{\perp\alpha}}{T_{\Pi\alpha}} - 1 \right] \tag{10}$$

For J = 0 the growth rate reduces to that given by Terashima [10].

5. Result and Discussions:

We have evaluated the dispersion relation, transverse energies and growth/damping rate of EIC waves in multi-component plasma. A graphical representation of the expressions is shown in Figures 1-9. The following parameters relevant to the plasma sheet boundary layer region Raikwar et al. [7 - 9].

B_0 = 400nT; Ω_{H^+} = 412 s^{-1}; Ω_{He^+} = 206 s^{-1} ; Ω_{0^+} = 51.50 s^{-1}; λ = 300m; E_1 = 50mV/m;

d_{lle} =52.55m

Using these data in derived expression for dispersion relation (Eq. 4), growth rate (Eq. 10), perpendicular resonant energy (Eq. 8) and parallel resonant energy (Eq. 9) we obtain the graphical representations.

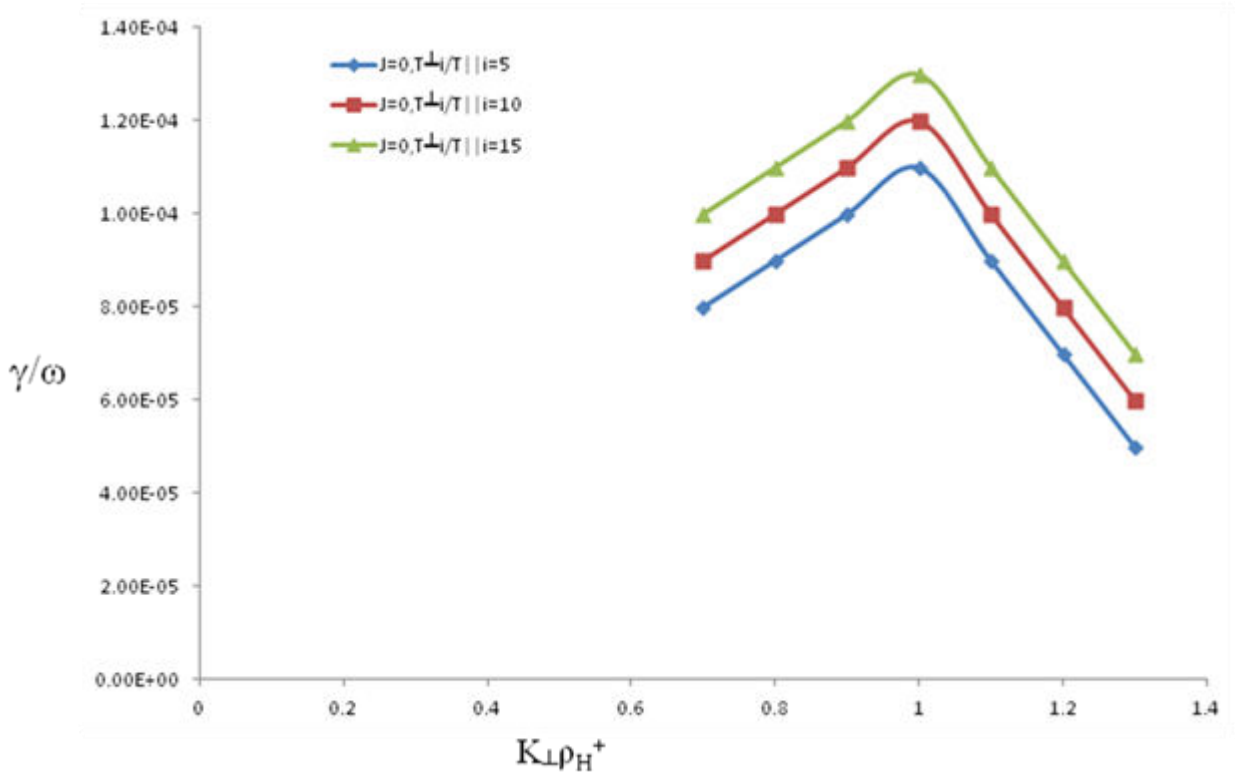

Figure 1: Variation of growth rate γ/ω versus $k_\perp \rho_{H^+}$ for Hydrogen ion at J = 0, for different temperature anisotropies $T_\perp/T_\parallel$ = 5, $T_\perp/T_\parallel$ = 10, $T_\perp/T_\parallel$ = 15

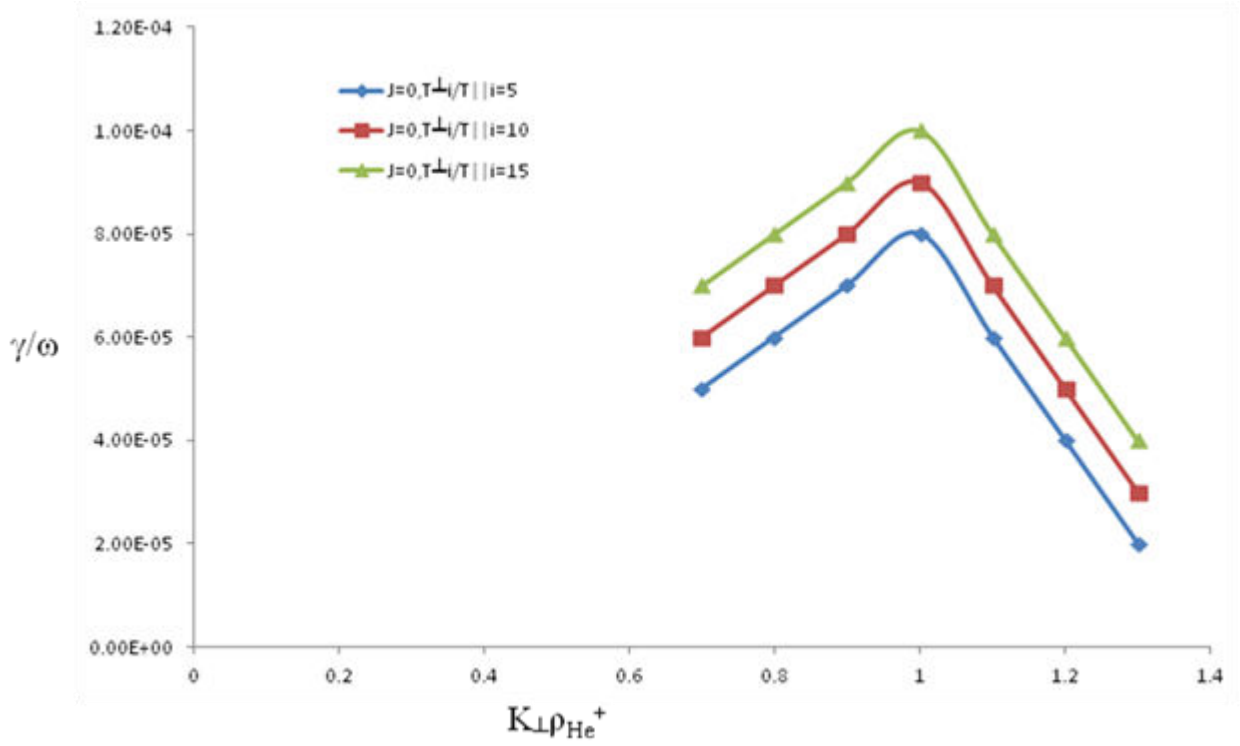

Figure 2: Variation of growth rate γ/ω versus $k_{\perp}\rho_{He^{+}}$ for Helium ion at J = 0, for different temperature anisotropies $T_{\perp}/T_{\parallel} = 5$, $T_{\perp}/T_{\parallel} = 10$, $T_{\perp}/T_{\parallel} = 15$

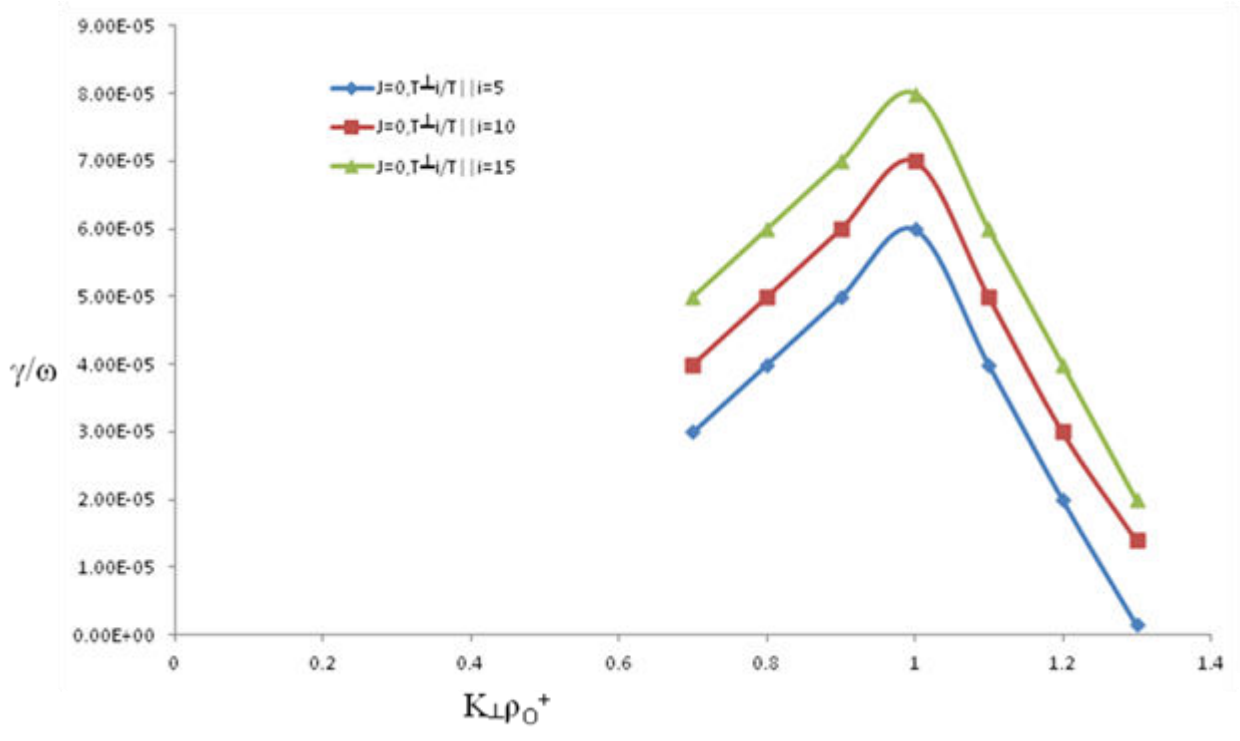

Figure 3: Variation of growth rate γ/ω versus $k_{\perp}\rho_{O^{+}}$ for Oxygen ion at J = 0, for different temperature anisotropies $T_{\perp}/T_{\parallel} = 5$, $T_{\perp}/T_{\parallel} = 10$, $T_{\perp}/T_{\parallel} = 15$

Figures 1-3 represent the variation of growth rate γ/ω verses perpendicular wave number for Hydrogen, Helium and Oxygen ions different temperature anisotropies $T_{\perp}/T_{\parallel} = 5$, $T_{\perp}/T_{\parallel} = 10$, $T_{\perp}/T_{\parallel} = 15$. It is observed that growth rate has increased with perpendicular wave number and temperature anisotropy for $K_{\perp}\rho_{\alpha}<1$ ($\alpha = H^{+}, He^{+}, O^{+}$);

and decreased for $K\perp\rho_\alpha>1$ for all the ions i.e. Hydrogen, Helium and Oxygen ions. It may be due to wave particle resonant interaction particles transfer energy to the wave which results as growth of the wave for region $K\perp\rho_\alpha<1$ on the other hand wave loses energy to the particles in the region $K\perp\rho_\alpha>1$, via wave particle resonance which results in reduction of growth rate. Growth rate is maximum when $K\perp\rho_\alpha$ is in the range of 1 because maximum energy exchange takes place at this point due to cyclotron resonance. It can also be concluded that growth rate is smaller for heavier ions i.e. Helium and Oxygen ions than lighter ion i.e. Hydrogen ion. This reduction of growth rate for heavier ions with respect to lighter ions may be due to the comparatively less transfer of energy by the heavier ions than the lighter ions. Above observation shows that growth rate of the wave is dependent on the temperature anisotropy as well as on heavier or lighter ions and perpendicular wave length in the particular region of interest i.e PSBL region. In PSBL temperature anisotropy plays an important role in plasma transport heating and large scale observed features particularly in transportation of cold plasma. Our results are analogous with Chaston et al. [11] which provide evidence for widespread heating of the ion plasma and Wing et al. [12] who showed that magneto sheath ions in the magnetosphere on the dawn side have significantly enhanced temperature. The amount of the ionospheric origin plasma population in the plasma sheet was found to be modulated by the geomagnetic and solar activity [13, 14] thus ionospheric plasma plays a role in the plasma sheet.

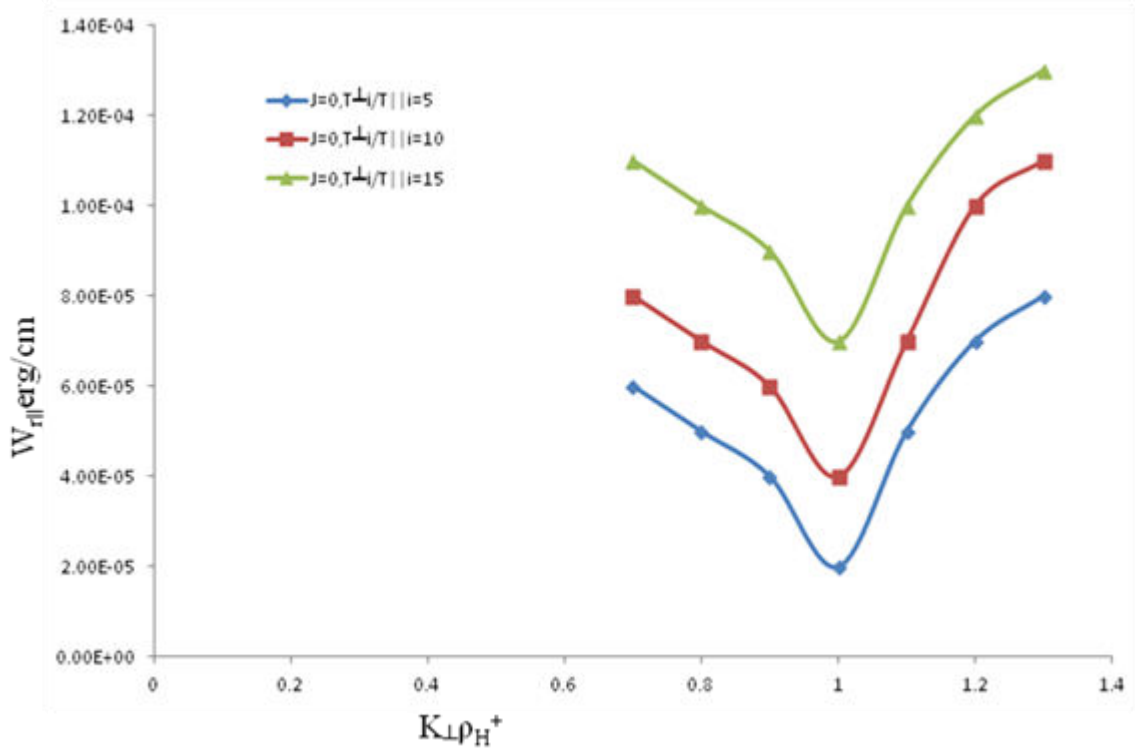

Figure 4: Variation of parallel resonant energy w_{rll} (erg/cm.) versus $k_\perp \rho_{H^+}$ for Hydrogen ion at J = 0, for different temperature anisotropies $T\perp/T_\parallel = 5$, $T\perp/T_\parallel = 10$, $T\perp/T_\parallel = 15$

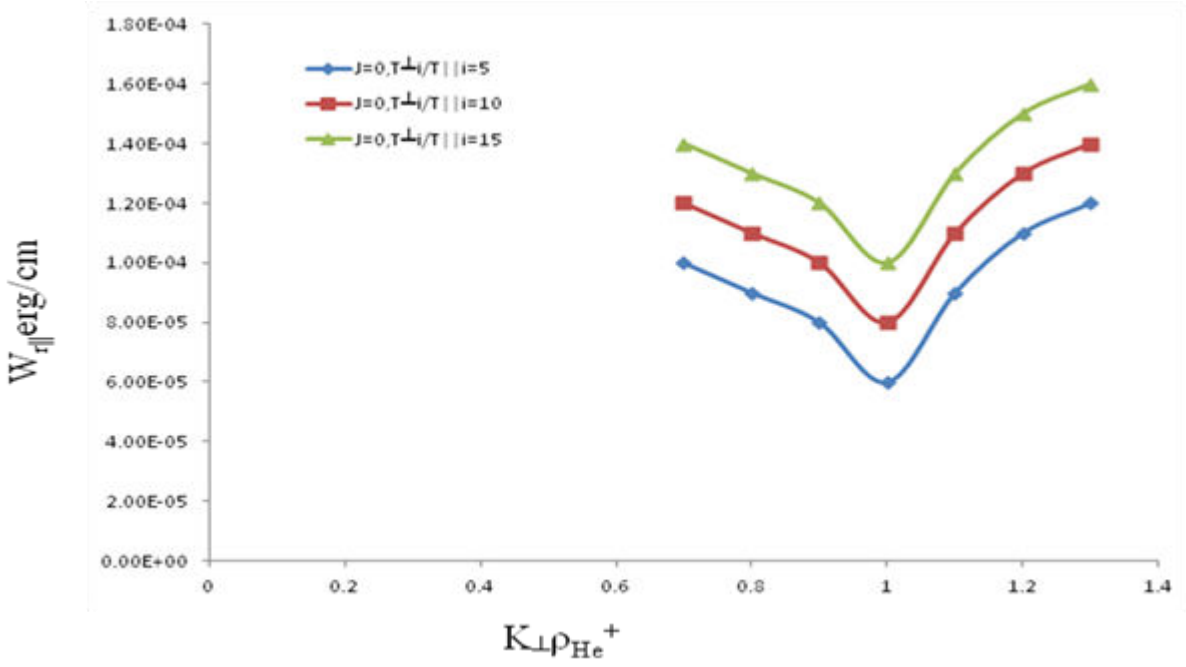

Figure 5: Variation of parallel resonant energy w_{rll} (erg/cm.) verses $k_{\perp}\rho_{He^+}$ for Helium ion at J = 0, for different temperature anisotropies $T_{\perp}/T_{\parallel} = 5$, $T_{\perp}/T_{\parallel} = 10$, $T_{\perp}/T_{\parallel} = 15$

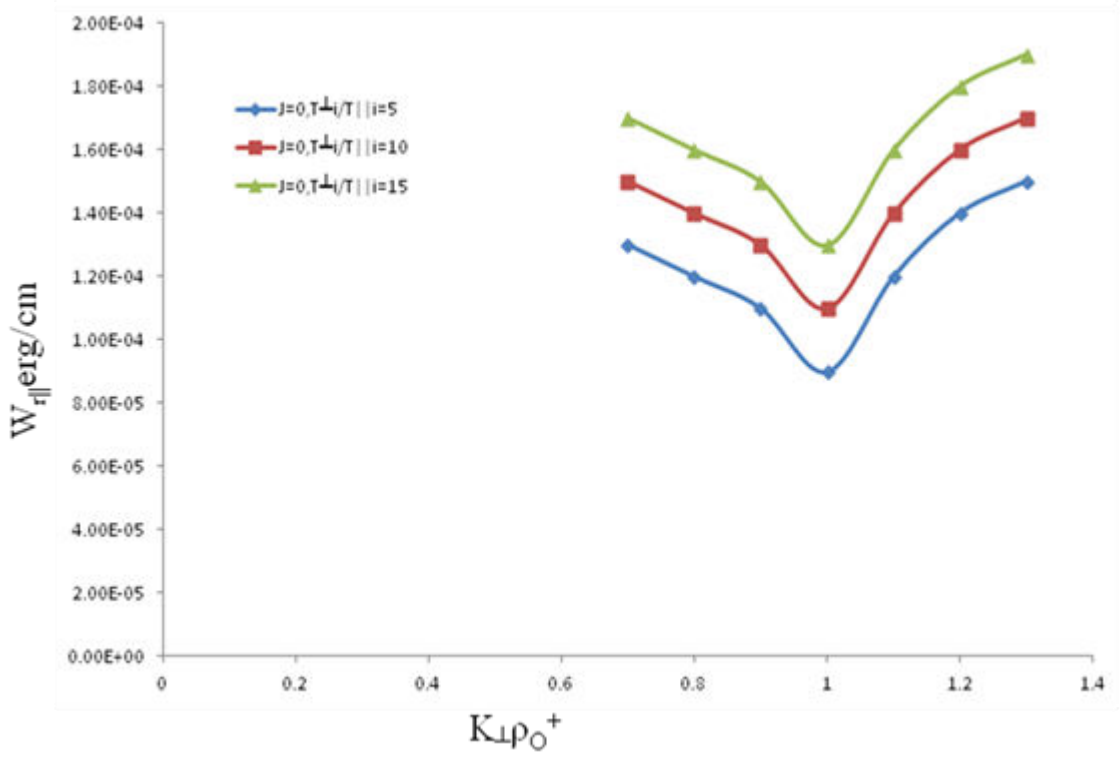

Figure 6: Variation of parallel resonant energy w_{rll} (erg/cm.) versus $k_{\perp}\rho_{O^+}$ for Oxygen ion at J = 0, for different temperature anisotropies $T_{\perp}/T_{\parallel} = 5$, $T_{\perp}/T_{\parallel} = 10$, $T_{\perp}/T_{\parallel} = 15$

Figures 4-6 depict the variation of parallel resonant energy $W_{r\parallel}$ (erg/cm.) verses $k_{\perp}\rho_i$ for Hydrogen, Helium and Oxygen ion for different temperature anisotropies $T_{\perp}/T_{\parallel} = 5$, $T_{\perp}/T_{\parallel} = 10$, $T_{\perp}/T_{\parallel} = 15$. It can be concluded that the parallel resonant energy of the particles decreases for $K_{\perp}\rho_{\alpha}<1$ because particles impart energy to the wave in this region via wave particle resonant interaction. At $K_{\perp}\rho_{\alpha}\sim1$ maximum energy exchange occurs because of cyclotron resonance. Parallel resonant energy again increases in the region $K_{\perp}\rho_{\alpha}>1$, in this region wave provides energy to the

particles by wave particle resonance interaction for all the ions i.e. Hydrogen, Helium and Oxygen ions which is supported by the reduction in growth rate of the wave. Our findings are supported by the Ahirwar et al. & Agrwal et al. [15]. It can also be observed that the temperature anisotropy enhances the parallel resonant energy which will also cause the heating of ions parallel to the magnetic field. Both hot and cold plasma have been observed to co-exist in the same region/field-line under all IMF conditions [12, 16]. The mechanisms for heating cold plasma, either solar wind or ionospheric origin, to hot plasma population has not been firmly established, but it does appear that the ion to electron temperature ratio (*Ti/Te*) is roughly conserved by the entry, energization, heating, and transport processes. This quasi "conserved" property deserves close and careful examinations, because it puts stringent constraints on the entry and heating mechanisms. Recently, Maggiolo and Kistler [13] found that O+ density increases with decreasing distance from the Earth and for magnetically active times and in the near Earth region, O+ density is higher at postmidnight than premidnight. This may be related to the presence of cold dense ions in the plasma sheet post-midnight sector after substorm onset [17, 18].

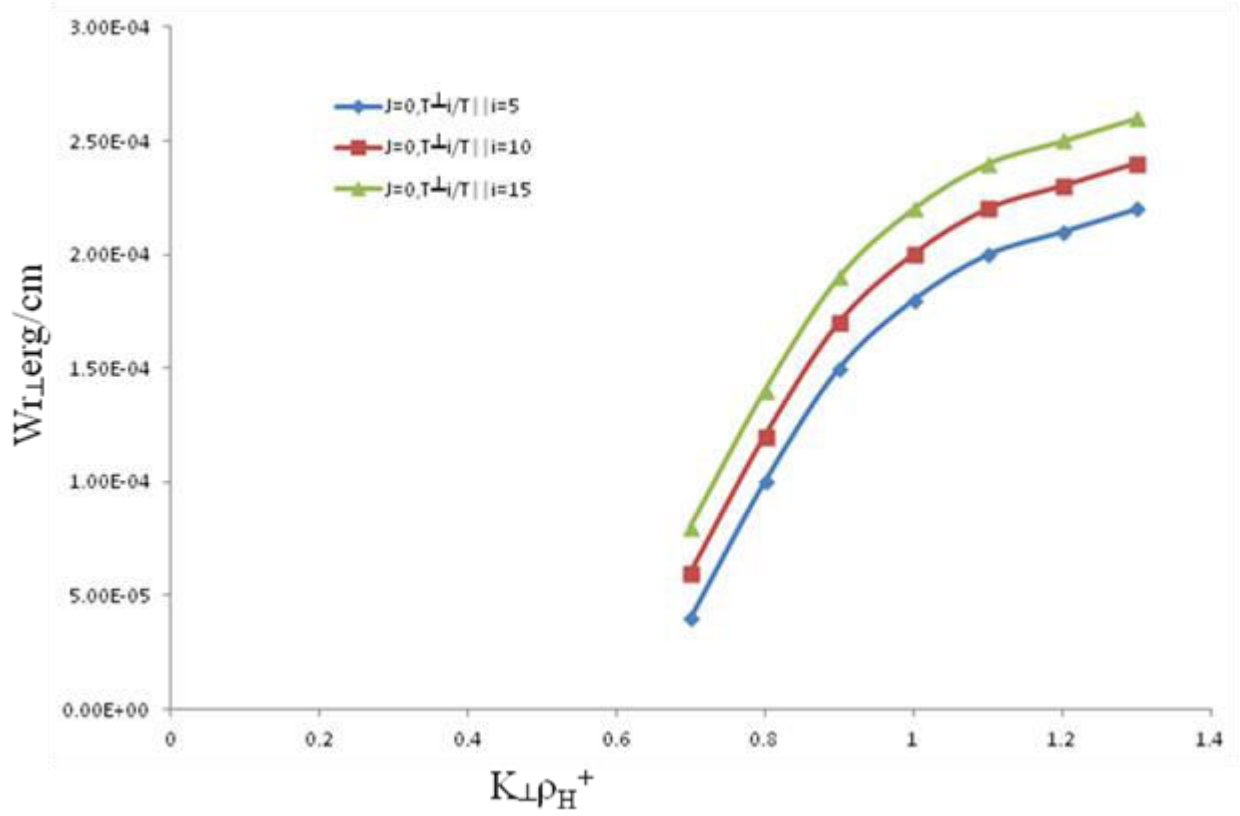

Figure 7: Variation of perpendicular resonant energy $w_{r\perp}$ (erg/cm.) verses $k_{\perp}\rho_{H^+}$ for Hydrogen ion at J = 0, for different temperature anisotropies $T\perp/T_{\parallel} = 5$, $T\perp/T_{\parallel} = 10$, $T\perp/T_{\parallel} = 15$

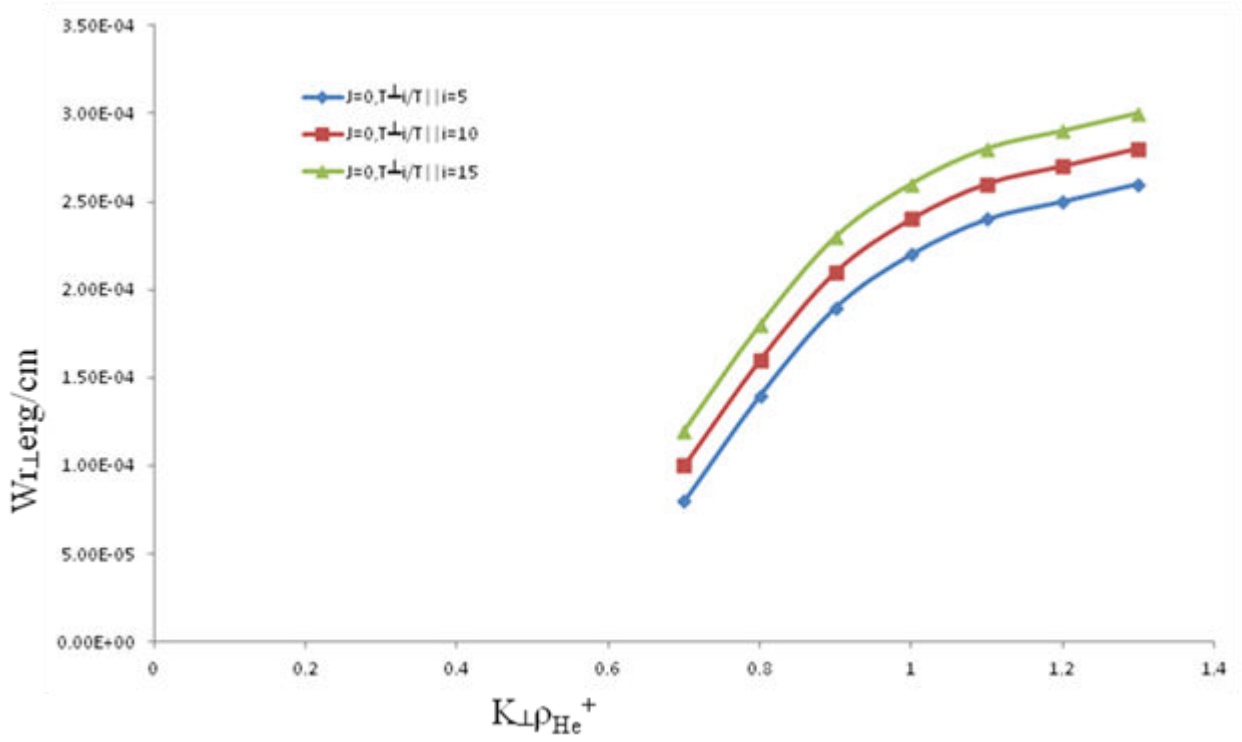

Figure 8: Variation of perpendicular resonant energy $w_{r\perp}$ (erg/cm.) verses $k_{\perp}\rho_{He^{+}}$ for Helium ion at J = 0, for different temperature anisotropies $T\perp/T_{\parallel} = 5$, $T\perp/T_{\parallel} = 10$, $T\perp/T_{\parallel} = 15$

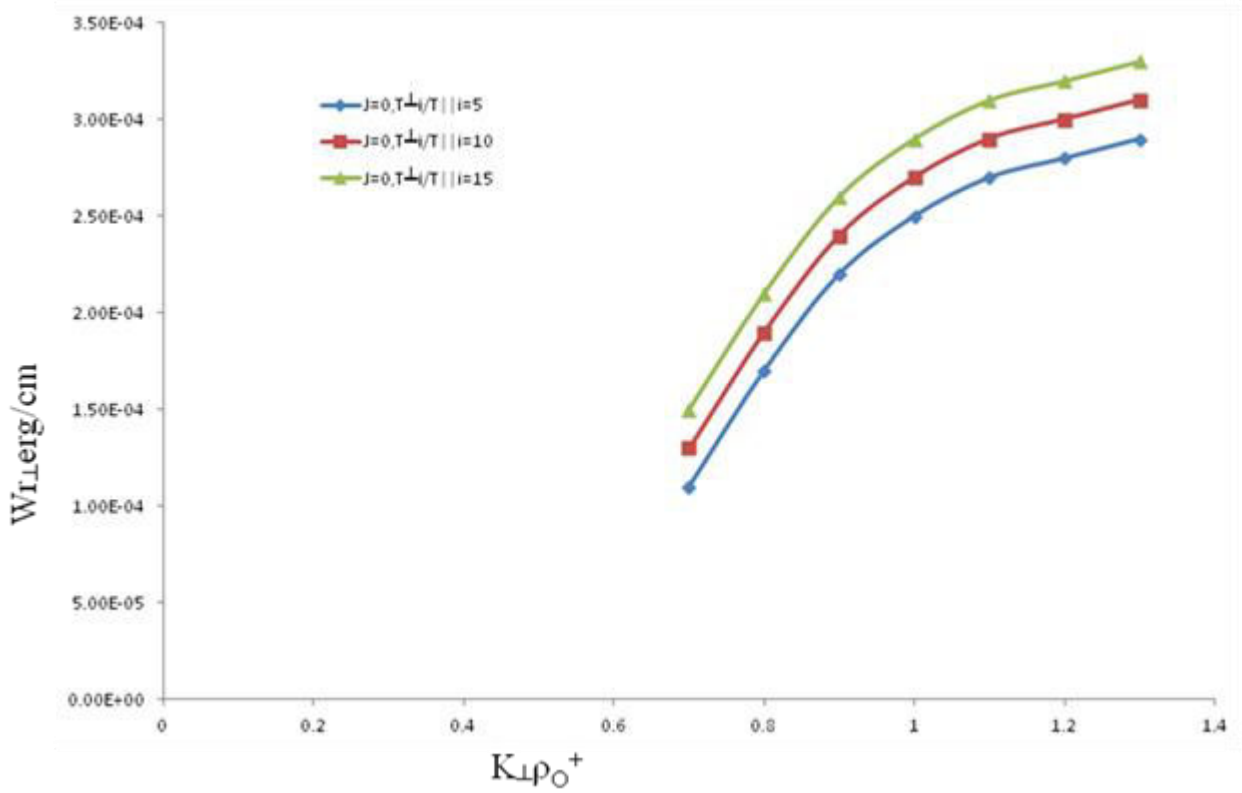

Figure 9: Variation of perpendicular resonant energy $w_{r\perp}$ (erg/cm.) verses $k_{\perp}\rho_{O^{+}}$ for Oxygen ion at J = 0, for different temperature anisotropies $T\perp/T_{\parallel} = 5$, $T\perp/T_{\parallel} = 10$, $T\perp/T_{\parallel} = 15$

Figures 7 – 9 depict the Variation of perpendicular resonant energy $w_{r\perp}$ (erg/cm.) verses $k_\perp \rho_i$ for Hydrogen, Helium and Oxygen ion at J = 0, for different temperature anisotropies $T\perp/T_\parallel = 5$, $T\perp/T_\parallel = 10$, $T\perp/T_\parallel = 15$. It can be concluded that perpendicular resonant energy for multi-ions enhance with the perpendicular wave number and temperature anisotropy. Hence the transverse acceleration to the magnetic field is possible due to wave particle resonance in which wave provides energy to the charged particles. Temperature anisotropy plays an important role in acceleration and heating of plasma which helps in plasma transport, can explain the large features seen in plasma sheet boundary layer region. This transverse acceleration can also play a significant role, particularly in the cold plasma transport from the flanks to the midnight meridian.

Finally it can be concluded that EIC turbulence (instability) is capable to transport plasma across magnetic boundaries, additionally electrons and ion heating is attributed to wave particle interaction or wave particle energy exchange. Such, turbulence is an important process that is intrinsic to the quasi-stable state of the tail and boundary layer [19], as well as its stability [20]. EIC waves also lead to nonlinear transverse plasma heating in PSBL region. Present study can be extended for storm times, which will be useful for the prediction of disturbances created during the Solar flares and CME'S. During these processes variations in magnetic field strength of earth's magnetosphere and charged particle density occurs. This can affect the electrostatic ion-cyclotron wave activity in PSBL region and may be applicable to other regions of earth's magnetosphere.

Acknowledgment: The author (PV) is thankful to ISRO and (BDR) is to UGC for financial assistance.

References

1. Kurian, M. J., Jyothi, S., Leju, S. K., Issak M., Venugopa, C., Renuka, G., 2009, Stability of electrostatic Ion-cyclotron waves in a multi-ion plasma, *J of Phys* 73, 1111.
2. Paschmann, G., Haaland, S., and Treumann, R., 2002, Auroral plasma physics, *Space Sci Rev,* 103, IX+.
3. Lavraud, B., Denton, M. H., Thomsen, M. F., Borovsky, J. E., Friedel, R. H. W., 2005, Superposed epoch analysis of dense plasma access to geosynchronous orbit, *Ann Geophys*, 23(7), 2519–2529.
4. Lavraud, B., Thomsen, M. F., Borovsky, J. E., Denton, M. H., Pulkkinen T. I., 2006b, Magnetosphere preconditioning under northward IMF: Evidence from the study of coronal mass ejection and corotating interaction region geoeffectiveness, *J Geophys Res*, 111, A09208, doi:10.1029/2005JA011566.
5. Keiling, A., 2006, Association of Pi2 pulsations and pulsed reconnection: Ground and Cluster observations in the tail lobe at 16 RE, *Ann Geophys*, 24, 3433.
6. Raikwar, B. D., Varma, P., Tiwari, M. S., 2015, Beam effects on electrostatic ion-cyclotron (EIC) wave with multi-ion plasma around cusp region, *Madhya Bharti J of Sci.* 59(2) 57-66.
7. Raikwar, B. D., Varma, P., Tiwari, M. S., 2016, Effect of density and general distribution function on electrostatic ion cyclotron waves with multi-ions plasma, *AJSIR* 1 21-34.
8. Raikwar, B. D., Varma, P., Tiwari, M. S., 2016, Study of general loss-cone distribution function on EIC waves with multi-ions plasma in PSBL region- particle aspect approach, *Astrn Space Sci*, 2 1-10.
9. Raikwar, B. D., Varma, P., Tiwari, M. S., 2016, Effect of temperature anisotropy an EIC waves with multi-ion plasma around PSBL region- particle aspect approach, *Proceedings 5th PSSI-PSC-2016*, ISBN-9788192657974, pp. 51-61.

10. Terashima, Y, 1967, 1967, Particle aspect analyses of electromagnetic and electrostatic instabilities due to anisotropic velocity distribution, *Prog Theor Phys(japan)*, 37, 661.

11. Chaston, C. C., Yao, Y., Lin, N., Salem, C., Ueno, G., 2013, Ion heating by broadband electromagnetic waves in the magnetosheath and across the magnetopause *J Geophys Res (Space Phys)* 118, 5579-5591, Doi: 10.1002/jgra.50506.

12. Wing, S., Johnson, J.R., Newell, P.T., Meng, C.I., 2005, Dawm-dusk asymmetries, ion spectra, and sources in the northward interplanetary magnetic field plasma sheet, *J Geophys Res* 110, A08205, Doi:10.1029/2005JA011086.

13. Maggiolo, R., Kistler, L.M., 2014, Spatial variation in the plasma sheet composition: dependence on geomagnetic and solar activity, *J Geophys Res Space Phys* 119, 2836–2857, doi:10.1002/2013JA019517.

14. Mouikis, C.G., Kistler, L.M., Liu, Y.H., Klecker, B., Korth, A., Dandouras, I., 2010, H+ and O+ content of the plasmasheet at 15–19 Re as a function of geomagnetic and solar activity, *J Geophys Res* 115, A00J16, doi:10.1029/2010JA015978.

15. Agarwal, P., Varma, P., Tiwari, M. S., 2011, Effects of density, temperature and velocity gradients on inertial Alfven wave in cusp region, *Planet. & Space Sci*, doi:10.1016/j.pss.2011.06.016.

16. Wang, C.P., Gkioulidou, M., Lyons, L.R., Angelopoulos, V., 2012, Spatial distributions of the ion to electron temperature ratio in the magnetosheath and plasma sheet, *J Geophys Res* 117, A08215, doi:10.1029/2012JA017658.

17. Wing, S., Gjerloev, J.W., Johnson, J.R., Hoffman, R.A., 2007, Substorm plasma sheet ion pressure profiles, *Geophys Res Lett* 34, L16110, doi:10.1029/2007GL030453.

18. Wing, S., Johnson, J.R.,2009, Substorm entropies, *J Geophys Res* 114, A00D07, doi:10.1029/ 2008JA013989

19. Antonova, E.E., 2005, The structure of the magnetospheric boundary layers and the magnetospheric turbulence, *Planet Space Sci* 53, 161–168, doi:10.1016/j.pss.2004.09.041.

20. Stepanova, M., Pinto, V, Valdivia, J.A., Antonova, E.E., 2011, Spatial distribution of the eddy diffusion coefficients in the plasma sheet during quiet time and substorms from THEMIS satellite data, *J Geophys Res* 116, A00I24, doi:10.1029/2010JA015887.